Supporting Information

Neubert et al. 10.1073/pnas.1000674107

SI Text Section 1

MEP Recording and Analysis. MEP recording and analysis procedures were identical for all experiments. Electromyographic (EMG) responses were recorded from the right hand FDI muscle using two surface Ag-AgCl electrodes in tendon-belly montage. An earth electrode was placed on the right elbow. EMG responses were band pass-filtered between 10 and 1,000 Hz, with an additional 50-Hz notch filter; sampled at 5,000 Hz; and recorded using a CED 1902 amplifier (Cambridge Electronic Design), a CED micro 1401 Mk.II A/D converter (Cambridge Electronic Design), and a personal computer running Spike2 (Cambridge Electronic Design). Analysis of these data concentrated on peak-to-peak amplitudes of the MEPs measured on TMS trials. Trials with incorrect responses, trials with premature (RT <150) responses, trials in which the test pulse failed to elicit a reliable MEP (amplitude <0.1 mV), and trials in which participants precontracted the FDI muscle before application of the TMS pulse (EMG amplitude >0.1 mV in the 80 ms before the pulse) were discarded from the analysis. Analyses of ppTMS/spTMS ratios were carried out based on the mean of the median normalized MEP amplitudes in each condition. Analyses of both behavioral and electrophysiological data were conducted using ANOVAs, utilizing repeated measures whenever possible. Significant effects were identified based on Huynh–Feldt-corrected ANOVA values, using SPSS 16.0 (SPSS, Inc.). Post hoc two-sided t tests were used to investigate significant effects in the ANOVAs further.

Even though trials with excessive precontraction of the right FDI muscle were discarded from the analyses, an additional analysis was performed on the remaining trials in the "right inferior frontal gyrus (rIFG)/M1 interaction experiment" to ensure that none of the reported MEP effects were caused by systematic differences in muscle contraction between conditions. The ANOVAs conducted on the MEP amplitudes were repeated for the values of the rms of the background EMG in the 80-ms interval before the application of the TMS pulses. None of the main effects and interactions significant in the MEP data reached significance when analyzing the rms. Therefore, MEP amplitude effects were not confounded with differences in FDI muscle contraction.

Coil Locations. The position of the test coil over the left M1 in all experiments was determined functionally. The coil was placed over the location that yielded the greatest MEP in the right hand FDI for a given intensity. In the "rIFG/M1 interaction" experiments, conditioning coil location in MNI space was, on average, ($x = 60$, $y = 14, z = 30$) and ($x = 60, y = 15, z = 29$) in the STAY and SWITCH experiments, respectively. In the experiments varying the IPLs between conditioning and test TMS pulses, mean rIFG conditioning coil location was ($x = 58, y = 15, z = 30$) (Fig. 1*D*).

The rIFG region identified with behavioral stopping is extensive (1), and its posterior part includes a region that we and others have frequently identified with PMv (2, 3). It was this region, immediately posterior to the ventral branch of the inferior precentral sulcus (4), and therefore close to the region studied by Swann et al. (5), that we studied. This region was chosen because (*i*) DW-MRI evidence in humans suggests that it is likely to be interconnected with STN (6), (*ii*) the only published tracer injection evidence for inferior frontal/STN connections in the monkey has come from this region's likely homolog (7), and (*iii*) functional MRI studies have indicated that cortex in this area is concerned with action inhibition and reprogramming even after controlling for various attentional demands (8). Of course, it remains a possibility that other rIFG and adjacent inferior frontal junction areas are concerned with other processes necessary for exerting cognitive control other than the inhibition of corticospinal excitability.

For the IPL experiment focusing on pre-SMA/M1 interactions, the conditional coil was placed over the medial frontal cortex at mean coordinates ($x = 1, y = 23, z = 60$). In the rTMS experiments, the pre-SMA repetitive TMS coil was placed at coordinates ($x = -1$, $y = 15, z = 71$) and the rIFG conditioning coil was placed at coordinates ($x = 59$, $y = 16$, $z = 25$). In the rTMS Pz control experiment, the repetitive TMS coil was placed over electrode Pz (9) at coordinates ($x = 0, y = 58, z = 77$) and the rIFG conditioning coil was placed at coordinates ($x = 58, y = 17, z = 23$).

SI Text Section 2

M1/M1 Control Experiment. To test whether changes in M1 excitability attributable to a conditioning pulse over rIFG could be explained by processes intrinsic to M1, we analyzed spTMS and ppTMS trial MEP data from an M1 control experiment, with both the conditioning and test pulses delivered through a coil placed over M1. This experiment focused on 175-ms SOA, where the rIFG/M1 interactions were strongest in the original rIFG/M1 interaction experiment. We investigated spTMS and ppTMS MEP effects during "switch" and "stay" trials. Experimental setup and stimulation parameters (pulse intensity, IPL) were exactly the same as in the previous two experiments, with the only difference being that both test pulses and conditioning pulses were applied to the same M1.

For the data from this M1 control experiment, an ANOVA on the FDI MEP ratios with within-subjects factors of hand (left vs. right hand response) and condition (switch vs. stay trial) revealed no significant effects. This indicates that the modulation of the MEP by the conditioning pulse is specific to the conditioning pulse being given over rIFG, because the effects are not replicated when the conditioning pulse is given over M1. Confirming this specificity, an ANOVA comparing MEP ratios between the switch trial data from the rIFG/M1 interaction experiment and the switch trials from the M1 control experiment with the within-subjects contrast hand and the between-subjects contrast area (conditioning pulse over rIFG vs. over M1) revealed a significant effect of area [$F(1,16) = 14.491$; $P = 0.002$]. Furthermore, an ANOVA comparing MEP ratios between the stay trials of the rIFG/M1 interaction experiment and the stay trials from the M1 control experiment with the within-subjects contrast hand and the between-subjects contrast area (conditioning pulse over rIFG vs. over M1) again revealed a significant between-subjects effect of area [$F(1,16) = 14.065$; $P = 0.002$]. Post hoc, one-sample t tests of the M1 control experiment MEP ratios against a baseline of 1.0 (or 100%) showed that the conditioning pulse over M1 led to global facilitation of the test pulse MEP amplitude in every condition (switch and stay, left and right hand responses). These results demonstrate that the rIFG/M1 interaction effects during action reprogramming and action execution trials cannot be explained by mechanisms intrinsic to M1.

It is known that stimulation of the motor cortex ipsilateral to the target muscle by a TMS conditioning pulse inhibits the size of the MEPs produced by test pulses over the contralateral motor cortex. This resting state effect is called interhemispheric inhibition (IHI). IHI of the contralateral M1 is obtained with IPLs of 7 ms or more and pulse intensities around the RMT. This type of inhibition is supposed to be mediated via transcallosal routes that have been localized with combined resting state ppTMS/diffusion-weighted (DW)-MRI techniques (10). It has been shown that IHI inhibits

I2 and I3 waves in the contralateral M1. M1/M1 interhemispheric connectivity was suggested to be involved in bimanual coordination. However, it seems implausible that M1/M1 functional interactions alone implement executive control during response switching and action reprogramming. Our results clearly suggest rIFG/M1 functional connectivity during response switching. Davare et al. (11) reported inhibitory interactions between a very similar area to the one we investigate and M1, at rest, within one hemisphere. Hence, IFG seems capable of inhibiting ipsilateral M1 as well as contralateral M1. Tracer studies in monkeys have shown direct connections between the premotor homolog of the area stimulated here and both ipsilateral and contralateral motor and premotor areas (12). Based on the relatively short IPL (8 ms) and the areas found in the TMS/DTI correlations (*SI Text* Section 6), we suggest that these effects are mediated via direct transcallosal rIFG/M1 pathways and, at longer latencies, possibly via rIFG/STN/M1 pathways. However, more research, especially on M1/M1 interactions during action reprogramming and response switching, needs to be conducted to answer this important question.

SI Text Section 3

Additional Data Analyses Relating to rIFG/M1 Interaction and IPL Experiments. The two rIFG/M1 interaction experiments investigated time courses of functional interactions between rIFG and M1 during action reprogramming (switch) and action execution (stay) trials. RIFG/M1 interactions during switch and stay trials were studied in two separate experiments involving different participants: the rIFG/M1 interaction switch experiment and the "rIFG/M1 stay experiment." This was necessary because obtaining an adequate number of both switch and stay trials with left and right hand responses, at three different SOAs, with both single and paired pulses would have resulted in (*i*) the participants receiving a very large number of TMS pulses and (*ii*) an exceedingly long experiment.

During the rIFG/M1 switch experiments, pulses (both single pulses to M1 and paired pulses to rIFG and M1 together) were almost exclusively delivered on switch trials [180 trials per block, 30 TMS trials (24 TMS trials per block delivered on switch trials, 6 TMS trials per block delivered on stay trials)] and only switch trial MEPs were analyzed. In the rIFG/M1 stay experiments, pulses were almost exclusively delivered on stay trials (24 TMS trials per block delivered on stay trials, 6 TMS trials per block delivered on stay trials) and only stay trial MEPs were analyzed. However, in the rIFG/M1 switch experiments, we delivered a small number ($n = 6$) of pulses on stay trials and administered a small number of switch trials (6) without TMS being delivered. A complimentary procedure was used in the stay experiment (24 TMS trials per block delivered on stay trials, 6 TMS trials per block delivered on switch trials). This prevented the subjects from reporting, on subsequent questioning, any relationship between trial type and TMS delivery.

However, perhaps the two most important points to note are, first, that the presence or absence of TMS could not serve as a precue indicating trial identity, because the pulses were only applied after the center color cue had already indicated a switch or stay trial. Second, it must be remembered that the focus of all analyses is the change in MEP size between single- and paired-pulse trials on a given trial type. Both the paired pulses on paired-pulse trials and the single pulses on single-pulse trials were delivered at the same time after central color cue onset. By calculating the ppTMS/spTMS MEP ratio, we were able to obtain M1 excitability changes attributable to an (artificial) activity burst in rIFG. Hence, by reporting MEP changes instead of absolute MEP values, we also control for general TMS-related effects.

The task was the same in all experiments. The main text reports the behavioral data in the rIFG/M1 interaction experiment, showing that participants responded slower and made more errors on switch trials as compared with stay trials, confirming the effectiveness of our experimental manipulation. These results were replicated in each of the other experiments: ANOVAs of median RTs in the two IPL experiments on correct trials and on error rates (incorrect responses/total number of trials) with "trial type" (switch vs. stay) and "experiment" (pre-SMA/M1 IPL experiment vs. rIFG/M1 IPL experiment) as within-subjects factors showed a main effect of trial type [$F(1,15) = 111.659$; $P < 0.001$ for RTs and $F(1,15) = 46.828$; $P < 0.001$ for error rates) but no main effect of experiment and no interaction between experiment and trial type ($P > 0.45$). A post hoc paired-samples t test on the behavioral data confirmed that subjects were significantly slower on switch trials than on stay trials (RT = 416.2 ms on switch vs. 302.5 ms on stay trials, $t(15) = 9.96$; $P < 0.001$) and made significantly more mistakes (error rate of 22.1% on switch trials vs. 2.1% on stay trials, $t(15) = 6.65$; $P < 0.001$). These behavioral results also replicate our previous study using this paradigm (13).

The experimental paradigm relies on the fact that participants prepare a response based on the sequence of color changes in the previous trials. Hence, switch and stay trials were defined on the basis of whether the central fixation took the same (stay) or different (switch) color as the previous trial, independent of which hand was actually used. An alternative way to classify switch and stay trials would be to classify them according to whether the hand used to make the response was the same ("motor stay") or different ("motor switch") as in the previous trial. To rule out the possibility that participants solved the task in this manner, we analyzed the behavioral and MEP data with the trials sorted according to these criteria. Analyzed in this way, the behavioral data showed no effect of condition (switch or stay) on RT or on error rate (both $P > 0.1$; Fig. S1 *A* and *B*). In addition, an ANOVA on the ppTMS/spTMS MEP ratios with the within-subjects factors of trial type (motor switch vs. motor stay), hand (left vs. right), and "SOA" (75, 125, and 175 ms) revealed a significant effect of SOA [$F(2,8) = 5.287$; $P = 0.034$] but no effect of trial type ($P = 0.504$) and no trial type × SOA interaction ($P = 0.642$). To investigate further whether there was any significant difference of ppTMS effects in any hand (left or right) at any given time point (75-, 125-, and 175-ms SOA) between motor switch and motor stay trials, we performed paired-samples t tests. These paired-samples t tests did not show any significant difference in rIFG/M1 interaction between motor switch and motor stay trials (all $P > 0.3$; Fig. S1). These results indicated that participants solved the task as we originally intended, by preparing their responses on the basis of previous cue colors and switching when these expectations were violated.

It is also very important to note that we recorded MEP data only from the right hand FDI muscle and applied M1 test pulses only to the left motor cortex. Hence, our analyses on rIFG/left M1 interactions during response switching and action reprogramming focus on MEP data from the right hand FDI muscle recorded on left and right hand response trials. Fig. 2 *A* and *B* shows ppTMS MEP changes from the right hand FDI muscle pooled over left and right hand responses. We pool the data over left and right hand responses because in both the pre-SMA/M1 SOA and the rIFG/M1 SOA experiments, we did not find a statistically significant effect of hand in the ANOVA on ppTMS/spMS MEP ratios with the within-subjects factors hand (left vs. right) and SOA (75, 125, and 175 ms) and the between-subjects factor condition (switch vs. stay). We used a one-sample two-tailed t test of the right hand FDI MEP ratios from left and right hand response switch trials (Fig. 2*A*) against baseline (MEP ratio of 1.0 or 100%) to analyze rIFG/M1 interactions during action reprogramming. When pooling left and right hand responses, we found significant inhibition of right hand FDI MEPs at 175-ms SOA [$t(9) = -3.578$; $P = 0.006$; Fig. 2*A*, asterisk] during action reprogramming. To check if this inhibition of right hand FDI MEPs was significant in both right and left hand response switch trials, we carried out

a one-sample one-tailed t test against a baseline of 1.0 (100%) for left and right hand responses separately. We found significant inhibition of right hand FDI MEPs for both left [$t(9) = 3.563$; $P = 0.003$] and right [$t(9) = 1.960$; $P = 0.041$] hand response trials. This does not, of course, necessarily mean that the rIFG/M1 interaction is identical during left and right hand responses. To follow up on this issue, we designed a more sensitive test for whether there are significant differences in the inhibitory influences exerted by rIFG on the motor cortex depending on whether the hand to be stopped is contralateral or ipsilateral to that motor cortex. We pooled data from the rIFG/M1 SOA experiment and rIFG/M1 IPL experiment from switch trials at 175-ms SOA with an IPL of 8 ms (rIFG/M1 SOA experiment) and 9 ms (rIFG/M1 IPL experiment), respectively. Data from 26 participants could be included in this analysis, and a paired-samples t test showed a significantly greater effect of rIFG/M1 inhibition at 175-ms SOA and 8- or 9-ms IPL when subjects were switching away from right hand (i.e., the hand contralateral to the stimulated M1) compared with left hand responses [$t(25) = -2.331$; $P = 0.028$]. However, because we do not find this significant difference between left and right hand responses in the rIFG/M1 interaction experiment alone, we present the data in Fig. 2*A* pooled over left and right hand responses.

SI Text Section 4

Additional Data Analyses for the Combined rTMS/ppTMS Experiments. Analysis of the behavioral data in the combined rTMS/ppTMS experiments indicates no effect of the rTMS stimulation on behavior. ANOVAs of median RTs on correct trials and of error rates with within-subjects factors trial type (switch vs. stay) and "rTMS" (before 1-Hz rTMS application to pre-SMA vs. after 1-Hz rTMS) and between-subjects factor experiment (pre-SMA rTMS experiment vs. Pz control experiment) showed a main effect of trial type [$F(1,12) = 96.714$; $P < 0.001$ for RTs and $F(1,12) = 22.865$; $P < 0.001$ for error rates] but no main effect of rTMS, no interaction between rTMS and trial type, no effect of experiment, and no interactions with the factor experiment ($P > 0.5$).

The changes in rIFG/M1 functional connectivity following 15 min of 1-Hz rTMS over pre-SMA reported in the main text were not present following 15 min of 1-Hz rTMS over the control site Pz. An ANOVA on the pre-SMA rTMS data with "pre/post" and trial type (switch vs. stay) as within-subjects factors shows a significant trial type × "pre/post interaction" [$F(1,7) = 11.918$; $P = 0.011$]. In an ANOVA with pre/post and trial type (switch vs. stay) as within-subjects factors and area (pre-SMA vs. Pz) as a between-subjects factor, we found a significant pre/post × area [$t(1,12) = 8.339$; $P = 0.014$] interaction. Testing the Pz results in an ANOVA with pre/post and trial type (switch vs. stay) as within-subjects factors showed a main effect of trial type [$F(1,5) = 7.931$; $P = 0.037$].

SI Text Section 5

DW-MRI and TBSS: Rationale and Validation. To elucidate the white matter pathways mediating the functional interactions between pre-SMA and rIFG on the one hand and M1 on the other hand, we used a TMS/FA correlation technique pioneered by Boorman et al. (14). The aim of this combination of methods is to find structural brain markers that correlate with a specific functional marker. In this case, the structural marker is the diffusion of water in a given voxel in the brain, as indexed by the FA. This is a useful index because it is known that water diffusion is directionally dependent in brain white matter. In a coherent fiber bundle, diffusion is less restricted along the fiber axis than across it; hence more diffusion will be measured along the fiber axis, resulting in a higher FA (15). Previous studies have demonstrated that this structural measure shows topographically specific correlations with certain skills, such as reading ability, visuospatial attention, or mental object rotation (16–19). Rather than correlating FA with a behavioral measure, we correlate it with the MEP ratio as an index of the functional interactions among brain regions. The rationale of the analysis is that a stronger white matter tract, as reflected in a higher FA value, results in a stronger influence of one brain region on another, as reflected in a higher MEP ratio.

Boorman et al. (14) validated this technique by looking at interactions between dorsal premotor cortex (PMd) and M1. It is well established that PMd is important for the selection of actions based on arbitrary learned stimulus-response mappings, referred to as conditional action selection, but not during simple action execution (20, 21). In macaques, PMd ablations influence conditional action selection but not simple action execution (22). In humans, imaging studies have shown strong increases in activity in PMd and the posterior parietal cortex during conditional as compared to simple action selection (23–25) and rTMS over PMd influences conditional action selection but not normal action execution (26). Consistent with these results, ppTMS studies have shown an influence of PMd on M1 that is especially prominent during conditional action selection (27, 28). Boorman et al. (14) then reasoned that these functional interactions should correlate with white matter pathways within the conditional action selection network. Correlating the physiological marker of functional interactions, the change in MEP, with individual differences in FA, these investigators indeed found the white matter tracts that are presumed to underlie these changes, including the white matter underlying PMd and the adjacent superior longitudinal fascicle connecting the intraparietal sulcus and premotor cortex. Their study thus demonstrated the feasibility of this method for investigating the relationship between structural measures of white matter density and physiological measures of functional interactions among brain regions. Following this early study, subsequent studies in different laboratories have used this technique to demonstrate the specificity of white matter tracts in the corpus callosum mediating interhemispheric interactions between the primary motor areas (10) and white matter circuits mediating parietal/M1 interactions during grasping (29), further demonstrating the specificity of the effects that can be obtained with this method. It is important to appreciate that the technique works because (*i*) subjects carry out the action reprogramming in a relatively consistent way even across several testing sessions and (*ii*) the effect of a given type of conditioning pulse in a given cognitive context is constant in a given subject (Fig. 2 and Fig. S2).

First, individual consistency in action reprogramming is revealed by comparing subjects' RTs on two occasions on which they performed the task. There was a very high correlation between the RTs recorded in the two IPL experiments (pre-SMA and rIFG IPL), even though at least 1 wk elapsed between experimental sessions, including significant correlations for RTs in general [$\rho = 0.891$, $P(16) < 0.001$], RTs in stay trials [$\rho = 0.840$, $P(16) < 0.001$], RTs in switch trials [$\rho = 0.899$, $P(16) < 0.001$], RT switching costs [difference in switch RTs and stay RTs: $\rho = 0.898$, $P(16) < 0.001$], and error switching costs [$\rho = 0.637$, $P(16) = 0.008$] (Fig. S2*A*). This suggests there are reliable individual differences in action reprogramming that may be attributable to individual differences in anatomical and functional networks of executive control and action reprogramming.

Second, individual consistency in the effects of conditioning pulses is revealed by comparing the modulating influences of the conditioning pulses on two occasions when conditioning was applied to the same brain region in the same behavioral context. We analyzed ppTMS/spTMS MEP ratios at 175-ms SOA and at 8- or 9-ms IPL as well as left and right hand responses from the (*i*) "rIFG/M1 SOA interaction experiment" (8-ms IPL, 175-ms SOA), (*ii*) rIFG/M1 IPL experiment (9-ms IPL, 175-ms SOA), (*iii*) "pre-SMA rTMS experiment" (rIFG/M1 connectivity before rTMS application: 8-ms IPL, 175-ms SOA), and (*iv*) "Pz rTMS control experiment" (rIFG/M1 connectivity before rTMS application: 8-ms IPL, 175-ms SOA). Altogether, 17 subjects participated in at least two of these four experiments, and could thus be included in the analysis. After rejection of two outliers using

Grubb's test, we found significant correlations for left hand response ppTMS/spTMS MEP ratios [$\rho = 0.689$, $P(15) = 0.002$] and right hand response MEP ratios [$\rho = 0.889$, $P(15) < 0.001$]. This also suggests high intraindividual test-retest reliabilities and very stable individual patterns of functional connectivity during action reprogramming and response switching (Fig. S2*B*).

SI Text Section 6

DW-MRI and TBSS: Data Acquisition and Analysis. DW-MRI data (three acquisitions of 60 directions, b-value = 1,000 s/mm^2, 2 × 2 × 2-mm voxels, 60 slices) were acquired from the 16 participants taking part in the rIFG/M1 and pre-SMA/M1 IPL experiments on a 3-T Siemens Trio MR scanner at the Oxford Centre for Clinical Magnetic Resonance (OCMR). Image analysis was carried out, and FA values were calculated with the Oxford Centre for Functional Magnetic Resonance Imaging of the Brain's (FMRIB) diffusion toolbox from FMRIB's Software Library (FSL) (30). We then performed TBSS (31, 32). Individual FA maps were aligned into standard space, and a mean FA image was created that underwent "skeletonization" so that only the centers of tracts (i.e., the maximal FA values) were spared and voxels with lower FA values were suppressed. Each participant's FA image was then projected onto this mean skeleton, which enabled statistical comparison of FA values from homologous regions of the FA map across participants. To test whether there was a relationship between functional connectivity, as found in the TMS experiment, and FA values across participants, we followed the procedure outlined by Boorman et al. (14) and previously used by Mars et al. (13) and Buch et al. (33). To test for local correlations between MEP effect size and FA values, we used permutation testing (34) as implemented in the FSL. Directionality of the effects was chosen such that we searched for correlations between FA and size of the MEP effect (i.e., increasing facilitation following pre-SMA stimulation and increasing inhibition following rIFG stimulation). Effects were reported as significant at a one-tailed statistical threshold of $P \leq 0.001$ (uncorrected). This threshold is similar to that used in many functional MRI studies, where the number of voxels, and thus the possibility of a false-positive result, is an order of magnitude greater. In addition, we note that it is not possible to use the correction for the multiple comparisons that are standard in functional neuroimaging studies because of the skeletal nature of the FA maps. As an extra precaution against false-positive results, we only report clusters with an extent of >10 voxels. These cutoffs are identical to those of Boorman et al. (14). All significant correlations between FA value and MEP effect were also significant at the cluster level and remained significant after partitioning out variance related to the possible confounding factors of participants' age and intensity of the test coil stimulation.

We investigated correlations between FA and functional interactions between rIFG/M1 and pre-SMA/M1 at both 6- and 12-ms IPLs in a single multiple regression analysis. A complete list of areas with significant correlations is reported in Table S1. These results indicated the involvement of direct cortical routes mediating rIFG/M1 and pre-SMA/M1 interactions at 6 ms and more indirect routes, including subcortical areas, at 12 ms. These conclusions are corroborated by contrasts illustrating the differential localization of areas of correlated FA in the 6-ms as compared with 12-ms IPLs, as shown in Table S2. White matter clusters correlating better with TMS effects at the 6-ms IPL were found exclusively in the major white matter tracts known to link cortical areas and subjacent to cortex, whereas clusters correlating better with TMS effects at the 12-ms IPL were found not just in similar regions but in deeper regions of white matter adjacent to the basal ganglia and around STN.

To investigate further the white matter tract to which these clusters belonged, we performed probabilistic diffusion tractography (PDT) (35) using either the rIFG [masks from the study of Tomassini et al. (3), kindly provided by the authors] or the right pre-SMA [masks from the study of Johansen-Berg et al. (36), kindly provided by the authors] as a seed mask and the individual clusters from the TBSS analysis as waypoints. In this way, we could investigate tracts originating from the rIFG of the pre-SMA and traveling through the clusters indicated to mediate our functional interaction effects. PDT estimates a probability distribution function on fiber direction at each voxel. A multifiber model was fit to the diffusion data at each voxel, allowing for the tracing of fibers through regions of fiber crossing or complexity. Here, we drew 1,000 streamline samples from our seed masks via the waypoint clusters to form an estimate of the probability distribution of connections from the masks via each individual waypoint cluster. The masks (pre-SMA and rIFG) and the correlated clusters identified with TBSS were transformed into each individual participant's space using the FSL nonlinear registration tool "FNIRT." PDT was run using the FSL PDT toolbox "Probtrackx" with 1,000 streamline samples, 2,000 steps per sample, a step length of 0.5 mm, and a curvature threshold of 0.2. When these streamlines reach a voxel in which more than one direction is estimated, they follow the direction that is closest to parallel with the direction at which the streamline arrives (if it does not exceed the curvature threshold). Tracts generated by PDT are volumes, wherein values at each voxel represent the number of samples (or streamlines) that passed through that voxel. For the elimination of spurious connections, tractography in individual subjects was thresholded to include only voxels through which at least 10 samples had passed [of 1,000 total samples; cf. Boorman et al. (14)]. These individual tracts were then binarized, transformed back into MNI standard space using FNIRT, and summed across subjects to produce group probability maps for each pathway. In these maps, each voxel value represents the number of subjects in whom the pathway passes through that voxel.

To quantify the probability of fibers reaching STN, we performed a ROI analysis. In each hemisphere, we defined the STN region as a box sized 10 × 10 × 10 mm that is centered at MNI coordinates ($x = \pm 10$, $y = -15$, $z = -5$) (1). For each individual participant and each cluster-derived tractography result, we determined the number of voxels that lay in the STN ROI. We then added together the number of ROI voxels for each condition (pre-SMA vs. rIFG: 6 vs. 12 ms). An ANOVA on the total number of ROI voxels with the within-subjects contrast of "IPL" (6 vs. 12 ms) and area (rFG vs. pre-SMA) revealed a significant effect of IPL [$F(1,15) = 252.084$; $P < 0.001$] and of area [$F(1,15) = 12.108$; $P = 0.003$]. To correct for number of FA clusters significantly correlated with TMS effects, we divided the total number of voxels in each condition by the number of clusters. An ANOVA on the "cluster-corrected" number of ROI voxels with the within-subjects contrast of IPL (6 vs. 12 ms) and area (rFG vs. pre-SMA) revealed a significant effect of IPL [$F(1,15) = 112.375$; $P < 0.001$] and a significant IPL × area interaction [$F(1,15) = 24.428$; $P < 0.001$]. Post hoc paired-samples t tests on the corrected number of ROI voxels confirmed that tractography derived from rIFG 12-ms IPL clusters rather than tractography derived from rIFG 6-ms IPL clusters [$t(15) = 2.701$; $P = 0.016$] and tractography derived from pre-SMA 12-ms IPL clusters reached the ROI significantly more often than tractography derived from pre-SMA 6-ms IPL clusters [$t(15) = 11.455$; $P < 0.001$]. There was also a significant difference between tractography derived from rIFG 6-ms IPL clusters and pre-SMA 6-ms IPL clusters [$t(15) = 4.775$; $P < 0.001$; rIFG > pre-SMA] and a significant difference between tractography results derived from rIFG 12-ms clusters and pre-SMA 12-ms clusters [$t(15) = -3.231$; $P = 0.006$; rIFG < pre-SMA]. However, these differences might also be driven by the "cluster correction," because we found the largest number of significantly correlated FA clusters in the rIFG 12-ms IPL condition (Table S1).

1. Aron AR, Poldrack RA (2006) Cortical and subcortical contributions to Stop signal response inhibition: Role of the subthalamic nucleus. *J Neurosci* 26:2424–2433.
2. Mayka MA, Corcos DM, Leurgans SE, Vaillancourt DE (2006) Three-dimensional locations and boundaries of motor and premotor cortices as defined by functional brain imaging: A meta-analysis. *NeuroImage* 31:1453–1474.
3. Tomassini V, et al. (2007) Diffusion-weighted imaging tractography-based parcellation of the human lateral premotor cortex identifies dorsal and ventral subregions with anatomical and functional specializations. *J Neurosci* 27:10259–10269.
4. Germann J, Robbins S, Halsband U, Petrides M (2005) Precentral sulcal complex of the human brain: Morphology and statistical probability maps. *J Comp Neurol* 493:334–356.
5. Swann N, et al. (2009) Intracranial EEG reveals a time- and frequency-specific role for the right inferior frontal gyrus and primary motor cortex in stopping initiated responses. *J Neurosci* 29:12675–12685.
6. Aron AR, Behrens TE, Smith S, Frank MJ, Poldrack RA (2007) Triangulating a cognitive control network using diffusion-weighted magnetic resonance imaging (MRI) and functional MRI. *J Neurosci* 27:3743–3752.
7. Nambu A, Tokuno H, Inase M, Takada M (1997) Corticosubthalamic input zones from forelimb representations of the dorsal and ventral divisions of the premotor cortex in the macaque monkey: Comparison with the input zones from the primary motor cortex and the supplementary motor area. *Neurosci Lett* 239:13–16.
8. Chikazoe J, et al. (2009) Functional dissociation in right inferior frontal cortex during performance of go/no-go task. *Cereb Cortex* 19:146–152.
9. Society AE; American Electroencephalographic Society (1994) Guideline thirteen: Guidelines for standard electrode position nomenclature. *J Clin Neurophysiol* 11:111–113.
10. Wahl M, et al. (2007) Human motor corpus callosum: Topography, somatotopy, and link between microstructure and function. *J Neurosci* 27:12132–12138.
11. Davare M, Lemon R, Olivier E (2008) Selective modulation of interactions between ventral premotor cortex and primary motor cortex during precision grasping in humans. *J Physiol* 586:2735–2742.
12. Dancause N, Barbay S, Frost SB, Mahnken JD, Nudo RJ (2007) Interhemispheric connections of the ventral premotor cortex in a new world primate. *J Comp Neurol* 505:701–715.
13. Mars RB, et al. (2009) Short-latency influence of medial frontal cortex on primary motor cortex during action selection under conflict. *J Neurosci* 29:6926–6931.
14. Boorman ED, O'Shea J, Sebastian C, Rushworth MF, Johansen-Berg H (2007) Individual differences in white-matter microstructure reflect variation in functional connectivity during choice. *Curr Biol* 17:1426–1431.
15. Johansen-Berg H, Rushworth MF (2009) Using diffusion imaging to study human connectional anatomy. *Annu Rev Neurosci* 32:75–94.
16. Klingberg T, et al. (2000) Microstructure of temporo-parietal white matter as a basis for reading ability: Evidence from diffusion tensor magnetic resonance imaging. *Neuron* 25:493–500.
17. Tuch DS, et al. (2005) Choice reaction time performance correlates with diffusion anisotropy in white matter pathways supporting visuospatial attention. *Proc Natl Acad Sci USA* 102:12212–12217.
18. Wolbers T, Schoell ED, Büchel C (2006) The predictive value of white matter organization in posterior parietal cortex for spatial visualization ability. *NeuroImage* 32:1450–1455.
19. Bengtsson SL, et al. (2005) Extensive piano practicing has regionally specific effects on white matter development. *Nat Neurosci* 8:1148–1150.
20. Wise SP, Murray EA (2000) Arbitrary associations between antecedents and actions. *Trends Neurosci* 23:271–276.
21. Passingham RE (1993) *The Frontal Lobes and Voluntary Action* (Oxford Univ Press, New York).
22. Halsband U, Passingham RE (1985) Premotor cortex and the conditions for movement in monkeys (Macaca fascicularis). *Behav Brain Res* 18:269–277.
23. Mars RB, Coles MG, Hulstijn W, Toni I (2008) Delay-related cerebral activity and motor preparation. *Cortex* 44:507–520.
24. Toni I, Passingham RE (1999) Prefrontal-basal ganglia pathways are involved in the learning of arbitrary visuomotor associations: A PET study. *Exp Brain Res* 127:19–32.
25. Toni I, Ramnani N, Josephs O, Ashburner J, Passingham RE (2001) Learning arbitrary visuomotor associations: Temporal dynamic of brain activity. *NeuroImage* 14: 1048–1057.
26. Schluter ND, Rushworth MFS, Passingham RE, Mills KR (1998) Temporary interference in human lateral premotor cortex suggests dominance for the selection of movements. A study using transcranial magnetic stimulation. *Brain* 121:785–799.
27. Koch G, et al. (2006) Time course of functional connectivity between dorsal premotor and contralateral motor cortex during movement selection. *J Neurosci* 26:7452–7459.
28. O'Shea J, Sebastian C, Boorman ED, Johansen-Berg H, Rushworth MF (2007) Functional specificity of human premotor-motor cortical interactions during action selection. *Eur J Neurosci* 26:2085–2095.
29. Koch G, et al. (2010) In vivo definition of parieto-motor connections involved in planning of grasping movements. *NeuroImage* 51:300–312.
30. Smith SM, et al. (2004) Advances in functional and structural MR image analysis and implementation as FSL. *NeuroImage* 23(Suppl 1):S208–S219.
31. Smith SM, et al. (2006) Tract-based spatial statistics: Voxelwise analysis of multi-subject diffusion data. *NeuroImage* 31:1487–1505.
32. Smith SM, et al. (2007) Acquisition and voxelwise analysis of multi-subject diffusion data with tract-based spatial statistics. *Nat Protoc* 2:499–503.
33. Buch ER, Mars RB, Boorman ED, Rushworth MF (2010) A network centered on ventral premotor cortex exerts both facilitatory and inhibitory control over primary motor cortex during action reprogramming. *J Neurosci* 30:1395–1401.
34. Nichols TE, Holmes AP (2002) Nonparametric permutation tests for functional neuroimaging: A primer with examples. *Hum Brain Mapp* 15:1–25.
35. Behrens TE, Berg HJ, Jbabdi S, Rushworth MF, Woolrich MW (2007) Probabilistic diffusion tractography with multiple fibre orientations: What can we gain? *NeuroImage* 34:144–155.
36. Johansen-Berg H, et al. (2004) Changes in connectivity profiles define functionally distinct regions in human medial frontal cortex. *Proc Natl Acad Sci USA* 101: 13335–13340.

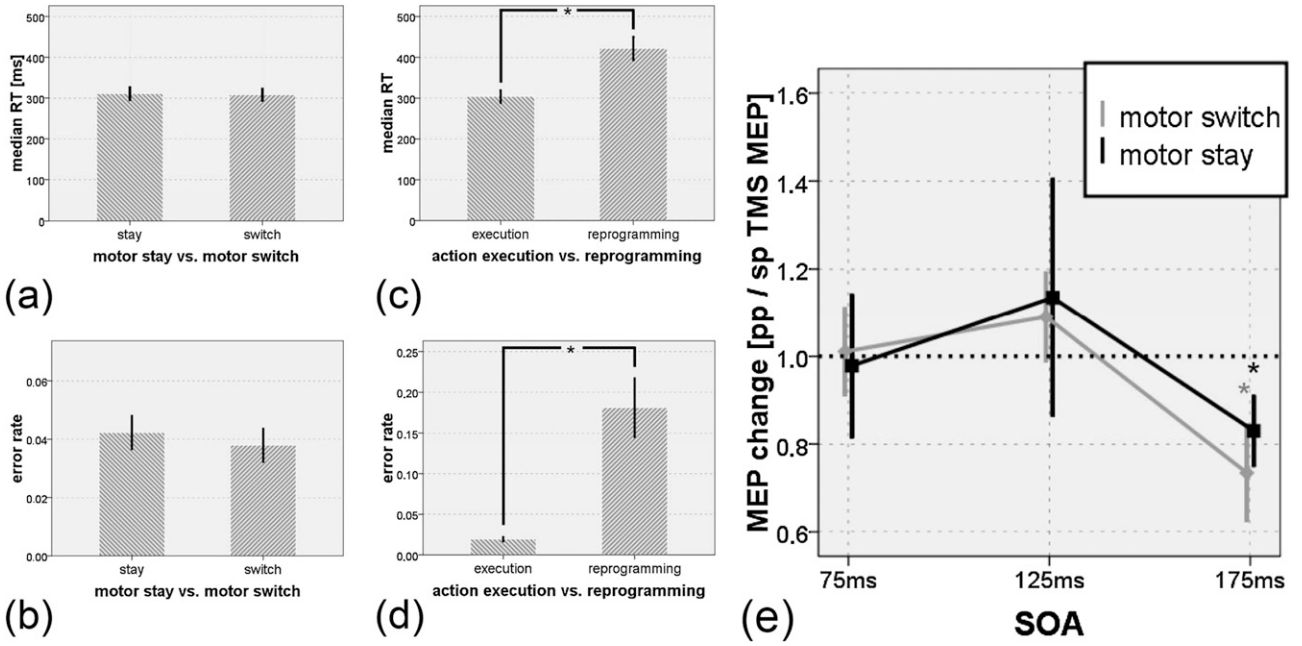

Fig. S1. Behavioral data from the rIFG/M1 interaction experiments. (*A*) Median RTs in motor switch and motor stay trials. (*B*) Error rates in motor switch and stay trials. Median RTs (*C*) and error rates (*D*) in action reprogramming and action execution trials. Asterisks indicate significant ($P < 0.05$) differences in a paired-samples *t* test. (Fig. 2*E*) Time course of rIFG/M1 interactions on color switch trials, separately for motor switch and stay trials. Asterisks indicate significant inhibition (significantly smaller than 1.0 in a one-sample one-tailed *t* test of MEP ratios).

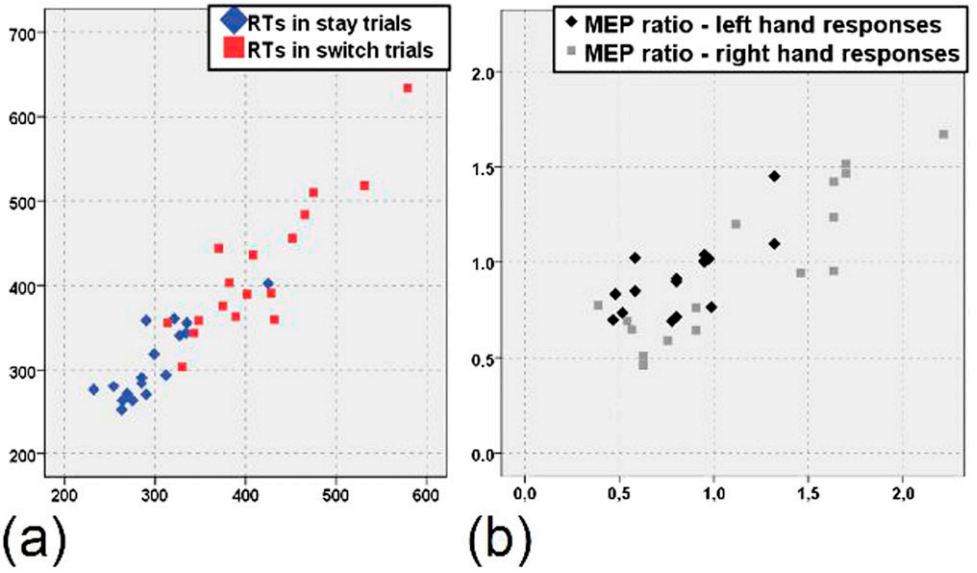

Fig. S2. Consistency of behavioral and TMS measures across experimental sessions. (*A*) Significant correlation for RTs at stay (red) and switch (blue) trials between rIFG/M1 IPL and pre-SMA/M1 IPL experiments. (*B*) Significant correlation between left and right hand response ppTMS/spTMS MEP ratios at 8- or 9-ms IPL and 175-ms SOA in different rIFG/M1 experiments.

Table S1. White matter clusters correlating with rIFG/M1 and pre-SMA/M1 functional interactions at 6- and 12-ms IPLs

Region	MNI coordinates			Cluster size (voxels)	Correlation (whole cluster)
	x	*y*	*z*		
rIFG/M1, 6-ms IPL					
White matter under rIFG	36	28	−7	10	**0.505**
White matter under rIFG/PMv	35	10	18	11	**0.508**
Dorsomedial white matter	−14	−27	60	10	**0.720**
rIFG/M1, 12-ms IPL					
White matter in the vicinity of STN	−19	−3	−10	**30**	0.588
White matter in the vicinity of STN	20	−4	−10	**14**	0.580
Extreme capsule	35	−12	−5	**19**	0.686
White matter underlying ventrolateral PFC	30	36	0	**18**	0.536
White matter underlying ventrolateral PFC	−30	35	8	**13**	0.517
Anterior PFC white matter	20	35	27	**28**	0.536
Anterior PFC white matter	−18	33	29	**32**	0.887
Superior longitudinal fascicle	36	−13	33	**17**	0.872
White matter underlying intraparietal sulcus	−31	−54	34	**11**	0.528
White matter underlying PMd	29	−8	44	**25**	0.718
White matter underlying PMd, pre-SMA	18	−3	46	**25**	0.649
White matter underlying pre-SMA	−9	29	52	**27**	0.620
White matter near M1	−18	−33	53	**26**	0.679
White matter near M1	21	−20	56	**14**	0.690
Pre-SMA, 6-ms IPL					
SLF III	−39	−26	31	**15**	0.652
Dorsomedial white matter	28	−18	36	**12**	0.582
Pre-SMA, 12-ms IPL					
White matter underlying anterior superior temporal sulcus	46	−7	−13	**17**	0.638
White matter adjacent to pallidum	−28	−20	−7	**11**	0.698
Dorsomedial white matter	−19	−4	36	**18**	0.708
Dorsomedial white matter	−21	4	36	**12**	0.663
White matter underlying intraparietal sulcus	−23	−48	39	**21**	0.638
Dorsomedial white matter	18	5	40	**54**	0.724

PFC, prefrontal cortex; PMv, ventral premotor cortex; SLF, Superior Longitudinal Fascicle.

Table S2. Differential white matter effects at 6- and 12-ms IPLs

Region	MNI coordinates			Cluster size (voxels)
	x	*y*	*z*	
(rIFG/M1, pre-SMA/M1) 6-ms IPL > (rIFG/M1, pre-SMA/M1) 12-ms IPL				
Anterior PFC white matter	−19	44	−8	17
White matter under rIFG	26	18	−1	48
White matter under rIFG	35	10	18	18
Dorsomedial white matter	37	−23	30	65
Dorsomedial white matter	−27	−23	29	12
White matter near M1	−47	−18	50	12
(rIFG/M1, pre-SMA/M1) 12-ms IPL > (rIFG/M1, pre-SMA/M1) 6-ms IPL				
White matter in the vicinity of STN	16	−2	−10	16
White matter in the vicinity of STN	−17	−22	−9	11
White matter under anterior rIFG	−30	36	0	18
White matter under rIFG	−45	10	13	12
White matter underlying pre-SMA	18	33	28	13
White matter underlying pre-SMA	−21	36	27	30
SLF	40	−5	32	14
White matter underlying intraparietal sulcus	22	−50	36	96
White matter near M1	−37	−16	34	16
White matter underlying per-SMA	−19	1	43	54
Dorsomedial white matter	17	−33	53	43
White matter near M1	−32	−14	52	13
White matter underlying pre-SMA	8	29	51	23